Proceedings of ALGORITMY 2009
pp. 1–10

REDUCED BASIS METHOD FOR FINITE VOLUME APPROXIMATION OF EVOLUTION EQUATIONS ON PARAMETRIZED GEOMETRIES

MARTIN DROHMANN*, BERNARD HAASDONK* AND MARIO OHLBERGER*

Abstract. In this paper we discuss parametrized partial differential equations (P^{2}DEs) for parameters that describe the geometry of the underlying problem. One can think of applications in control theory and optimization which depend on time-consuming parameter-studies of such problems. Therefore, we want to reduce the order of complexity of the numerical simulations for such P^{2}DEs. Reduced Basis (RB) methods are a means to achieve this goal. These methods have gained popularity over the last few years for model reduction of finite element approximations of elliptic and instationary parabolic equations.

We present a RB method for parabolic problems with general geometry parameterization and finite volume (FV) approximations. After a mapping on a reference domain, the parabolic equation leads to a convection-diffusion-reaction equation with anisotropic diffusion tensor. Suitable FV schemes with gradient reconstruction allow to discretize such problems. A model reduction of the resulting numerical scheme can be obtained by an RB technique. We present experimental results, that demonstrate the applicability of the RB method, in particular the computational acceleration.

Key words. Reduced basis methods, model reduction, geometry transformation, heat equation

AMS subject classifications. 76M12, 76R50, 35K05

1. Introduction. In this paper, we present a model reduction recipe for the numerical solution of evolution equations on parametrized geometries. For this purpose we introduce a parameter μ from a parameter set $\mathcal{P} \subset \mathbb{R}^p$ into the problem equation. In applications these parameters can characterize certain properties of the physical model which affect initial and boundary data, the evolution equation or, as our current new focus, the geometry of the domain. In general, such a *parametrized partial differential equation* (P^{2}DE) can be written as

$$\partial_t u(t;\mu) - \mathcal{L}(t;\mu)[u(t;\mu)] = 0 \qquad \text{in } \Omega(\mu) \times [0, T_{\max}] \tag{1.1}$$

with bounded domains $\Omega(\mu) \subset \mathbf{R}^d$ for all $\mu \in \mathcal{P}$ and additional initial and boundary conditions.

Computational schemes give us solutions $\{U_H^k(\mu)\}_{k=0}^K$ of such a P^{2}DE that approximate $u(t^k;\mu)$ at time instants $0 = t^0 < \cdots < t^K = T_{\max}$. These approximations are from a high-dimensional vector space $\mathcal{W}_H(\mu) \subset L^2(\Omega(\mu))$ and their computation for many different parameters can be very time consuming. The idea applied in this presentation is therefore to further approximate the snapshots by reduced solutions $\{U_N^k\}_{k=0}^K$ from a low dimensional *reduced basis space* $\mathcal{W}_N \subset \mathcal{W}_H$. The construction of a reduced basis space is time expensive by itself, but it allows fast computations of the reduced solutions afterwards. Reduced Basis (RB) methods have gained popularity in the last few years. They have successfully been applied on finite element (FE) schemes for elliptic and parabolic problems. A general overview of these methods can be found in [8]. Recently, we presented RB methods for two kind of finite volume (FV) schemes:

*University of Münster, Institute for Numerical and Applied Mathematics, Einsteinstr. 62, 48149 Münster, Germany (mdroh_01@wwu.de, bhaas_01@wwu.de, mario.ohlberger@wwu.de)

first to those that have an *affine parameter dependence* [6] and second for evolution equations with an explicit discretization but general parameter dependence [7].

In this presentation, we want to focus on the geometric parametrization which is a new field for RB methods applied to FV discretizations. In [10] the applicability of an RB method for a FE discretization of flow problems on parametrized geometries is already demonstrated, but this approach assumes the solution to be globally continuous and is therefore not applicable in the FV context. In our approach, the evolution equation is transformed onto a reference domain and the non-affine reference transformation hereby introduces new terms that depend in a non-affine way on the parameter. Therefore, the discretization operator needs to be approximated by a so-called *empirical interpolation* [1]. The current presentation is based on the thesis [3] which contains more details on the present study.

The structure of the paper is as follows. Section 2 presents the parametrized diffusion equation, its reformulation on a reference domain, the FV discretization and the reduced basis method. Section 3 gives experimental results which demonstrate the applicability of the model reduction technique. We conclude and give some perspectives in Sec. 4.

2. Reduced Basis Method for the Parametrized Heat Equation. We focus on a two dimensional instationary heat equation as a model problem. We present its reformulation on a reference domain, which results in a convection-diffusion-reaction equation with (in general) anisotropic diffusion tensor. This can be discretized with finite volume schemes using suitable gradient reconstruction techniques. Subsequently, this finite volume scheme can be treated by a RB method after a so called empirical interpolation of the finite volume space operator.

2.1. Geometry Transformation. For every $\mu \in \mathcal{P}$ we want to determine a solution $u(x,t;\mu)$ on a polygonal domain $\Omega(\mu) \subset \mathbb{R}^2$ for all times $t \in \mathbf{T} := [0, T_{\max}], T_{\max} > 0$, which satisfies the equations

$$\begin{aligned} \partial_t u(x,t;\mu) - a(\mu)\Delta u(x,t;\mu) &= 0 && \text{in } \Omega(\mu)\times\mathbf{T} \\ u(x,t;\mu) &= u_D(x,t;\mu) && \text{on } \Omega_D(\mu)\times\mathbf{T} \\ \nabla u(x,t;\mu)\cdot\mathbf{n} &= 0 && \text{on } \Omega_N(\mu)\times\mathbf{T} \\ u(x,0;\mu) &= u_0(x;\mu) && \text{in } \Omega(\mu). \end{aligned} \tag{2.1}$$

In these equations the functions u_0 and u_D represent initial data and Dirichlet boundary conditions.

We select an arbitrary parameter $\hat{\mu} \in \mathcal{P}$ that defines the reference domain $\hat{\Omega} := \Omega(\hat{\mu})$. It will be assumed that for every domain $\Omega(\mu)$, there exists a diffeomorph map $\Phi(\mu) : \hat{\Omega} \to \Omega(\mu)$. The heat equation given in (2.1) can then, for every $\mu \in \mathcal{P}$, be transformed onto the reference domain $\hat{\Omega}$.

LEMMA 2.1 (Geometry transformation). *Let u be a solution of (2.1). Then the function $\hat{u}(\hat{x},t) := u(\Phi(\hat{x}),t;\mu)$, with coordinates $\hat{x} := \Phi^{-1}(x)$ on the reference domain, is a solution of the equivalent convection–diffusion–reaction equation*

$$\partial_t \hat{u} - a(\mu)\nabla_{\hat{x}}\cdot(GG^t\nabla_{\hat{x}}\hat{u}) + a(\mu)\nabla_{\hat{x}}\cdot(v\hat{u}) - a(\mu)(\nabla_{\hat{x}}\cdot v)\hat{u} = 0 \qquad \text{in } \hat{\Omega}\times\mathbf{T}. \tag{2.2}$$

Here, we used the abbreviations

$$\tilde{v}(\hat{x}) := \begin{pmatrix} \partial_{\hat{x}_1} G_{11}(\hat{x}) & \partial_{\hat{x}_1} G_{12}(\hat{x}) \\ \partial_{\hat{x}_2} G_{21}(\hat{x}) & \partial_{\hat{x}_2} G_{22}(\hat{x}) \end{pmatrix} \begin{pmatrix} 1 \\ 1 \end{pmatrix} \tag{2.3}$$

$$v(\hat{x}) := G(\hat{x})\tilde{v}(\hat{x}), \tag{2.4}$$

with $G(\hat{x}) = \big(G_{ij}(\hat{x})\big)_{i,j=1,2}$ *being the Jacobi matrix of the inverse geometry transformation*

$$G(\hat{x}) := D\Phi^{-1}|_{\Phi(\hat{x})}. \tag{2.5}$$

Proof. The transformation affects only the space dependent part of the equation, such that we can concentrate on the diffusion term. Repeated use of the chain rule yields

$$\begin{aligned} a(\mu)\nabla_x \cdot (\nabla_x u) &= a(\mu)\nabla_x \cdot (G^t \nabla_{\hat{x}} \hat{u}) \\ &= a(\mu)(G^t \nabla_{\hat{x}}) \cdot (G^t \nabla_{\hat{x}} \hat{u}). \end{aligned} \tag{2.6}$$

In order to bring this differential equation into the form of a convection–diffusion–reaction equation we rewrite the diffusion term of (2.2) using the notation $G_{i\cdot}$ for the i-th row of G

$$\begin{aligned} a(\mu)\nabla_{\hat{x}} \cdot (GG^t \nabla_{\hat{x}} \hat{u}) &= a(\mu) \sum_{i=1}^{2} \partial_{\hat{x}_i} (G_{i\cdot} \cdot G^t \nabla_{\hat{x}} \hat{u}) \\ &= a(\mu) \sum_{i=1}^{2} (\partial_{\hat{x}_i} G_{i\cdot}) \cdot G^t \nabla_{\hat{x}} \hat{u} + a(\mu) \sum_{i=1}^{2} G_{i\cdot} \cdot \partial_{\hat{x}_i} (G^t \nabla_{\hat{x}} \hat{u}) \\ &= a(\mu) \begin{pmatrix} \partial_{\hat{x}_1} G_{11}(\hat{x}) & \partial_{\hat{x}_1} G_{12}(\hat{x}) \\ \partial_{\hat{x}_2} G_{21}(\hat{x}) & \partial_{\hat{x}_2} G_{22}(\hat{x}) \end{pmatrix} \begin{pmatrix} 1 \\ 1 \end{pmatrix} \cdot G^t \nabla_{\hat{x}} \hat{u} \\ &\quad + \underbrace{a(\mu)(G^t \nabla_{\hat{x}}) \cdot (G^t \nabla_{\hat{x}} \hat{u})}_{=\text{RHS of (2.6)}}. \end{aligned} \tag{2.7}$$

If we now insert (2.7) into (2.6), we end up with the stated result

$$\begin{aligned} a(\mu)\nabla_x \cdot \nabla_x u &= a(\mu)\nabla_{\hat{x}} \cdot (GG^t \nabla_{\hat{x}} \hat{u}) - a(\mu)\tilde{v} \cdot G^t \nabla_{\hat{x}} \hat{u} \\ &= a(\mu)\nabla_{\hat{x}} \cdot (GG^t \nabla_{\hat{x}} \hat{u}) - a(\mu) G\tilde{v} \cdot \nabla_{\hat{x}} \hat{u} \\ &= a(\mu)\nabla_{\hat{x}} \cdot (GG^t \nabla_{\hat{x}} \hat{u}) - a(\mu)\nabla_{\hat{x}} \cdot (v\hat{u}) + a(\mu)(\nabla_{\hat{x}} \cdot v)\hat{u}. \end{aligned} \tag{2.8}$$

□

Note in particular, that we get a pure diffusion equation, if the transformation map $\Phi(\mu)$ is an affine mapping, that is, it can be written in the form $\Phi(x;\mu) = A(\mu)x + b(\mu)$ with a map A that is linear in x and a vector $b(\mu)$. Then the second derivative vanishes and as a consequence v equals zero and so do the convection and the reaction terms in equation (2.2). Other RB approaches for problems with a geometry parametrization that are based on FEM discretization therefore use decompositions of the domain with piecewise affine mappings [9]. We remark, that the concept cannot be easily transferred to Finite Volume schemes, as the consistency of the numerical fluxes introduces a coupling between the subdomains.

2.2. Finite Volume Discretization. The numerical scheme which we now choose for the discretization of (2.2) is an explicit Finite Volume scheme of first order. The diffusion term leads to small time step sizes, and an implicit scheme would be preferable. As the RB methodology, however, is based on the availability of localized operators, it is not directly transferable to implicit discretizations.

We assume the reference domain to be rectangular in order to use a uniform Cartesian grid. This allows us to use the approach introduced by [2] for discretization of the anisotropic diffusion tensor GG^t in (2.2). Let us remark, however, that a discretization on an unstructured grid, e.g. proposed in [4], would be compatible with the further exposition.

The time domain is discretized uniformly into $K+1$ time steps of time step size $\Delta t := \frac{T_{\max}}{K}$ and time instants $t^k := k\Delta t$ for $k = 0, \dots, K$. We use a tessellation $\mathcal{T} := \{e_i\}_{i=1}^H$ of the domain Ω consisting of disjoint, equally sized, rectangular elements e_i, such that $\bar{\Omega} = \bigcup_{i=1}^H \bar{e_i}$. On this grid we define elementwise constant functions which build the high dimensional discrete function space $\mathcal{W}_H := \operatorname{span}\{\chi_{e_i} \mid e_i \in \mathcal{T}\}$. For every element e_i, we introduce the notations $\mathcal{N}(i,j)$ for the index of the element's j-th neighbour cell and σ_{ij} respectively $\mathbf{n}_{ij}$ for the corresponding edges and outer normals, with $j = 0, \dots, 3$ indicating right, upper, left and lower neighbourship. For simplicity, the boundary conditions are handled by using the concept of ghost-cells. If σ_{ij} is an interior edge, i.e. $\sigma_{ij} \not\subset \partial\Omega$, we denote the line connecting the two barycenters of the two cells neighbouring σ_{ij} by s_{ij}. Furthermore, for these interior edges, we define the end-points by x_{ij}^k, $k = 0, 1$. Then, we use $\mathcal{N}^k(i,j)$ as index sets containing the indices of the 4 cells adjacent to x_{ij}^k. With this notation, the explicit Finite Volume scheme

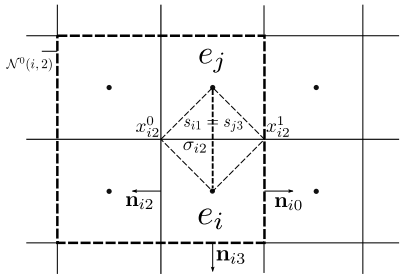

Fig. 2.1: Part of the grid with notations used in this paper, with $j := \mathcal{N}(i,2)$.

produces the discrete solutions $U_H^k(x;\mu) = \sum_{i=1}^H U_i^k(\mu)\chi_{e_i}(x) \in \mathcal{W}_H$, for $k = 0, \dots, K$ and $\mu \in \mathcal{P}$ by evaluating the recursion

$$U_i^0(\mu) = \frac{1}{|e_i|}\int_{e_i} u_0(\mu), \qquad U_i^{k+1}(\mu) = U_i^k(\mu) - \frac{\Delta t}{|e_i|}\sum_{j=0}^{3} g_{ij}(U_H^k(\mu)), \tag{2.9}$$

where g_{ij} denote the numerical flux functions. We choose a numerical flux with upwinding for the convective term and define g_{ij} for interior edges by

$$\begin{aligned} g_{ij}(U_H^k(\mu)) :=& |\sigma_{ij}| a(\mu)\big(GG^t\mathcal{R}(\sigma_{ij}, U_H^k(\mu)) \\ &+ vU_i^k(\mu)\cdot\mathbf{n}_{ij}\ \chi_{\{v\cdot\mathbf{n}_{ij}>0\}} + vU_j^k(\mu)\cdot\mathbf{n}_{ij}\ \chi_{\{v\cdot\mathbf{n}_{ij}<0\}}\big) \\ &+ a(\mu)\int_{e_i}(\nabla\cdot v)\ U_i^k(\mu), \end{aligned} \tag{2.10}$$

where the continuous functions and operators are evaluated at the barycenter of the edge σ_{ij} and $\mathcal{R}$ denotes the reconstruction operator for the gradient given by

$$\begin{aligned}\mathcal{R}(\sigma_{ij}, U_H^k(\mu)) =& \frac{1}{|s_{ij}|}(U_j^k(\mu) - U_i^k(\mu))\mathbf{n}_{ij} \\ &+ \frac{1}{4|\sigma_{ij}|}\left(\sum_{l\in\mathcal{N}^0(i,j)} U_l^k(\mu) - \sum_{l\in\mathcal{N}^1(i,j)} U_l^k(\mu)\right)\mathbf{t}_{ij},\end{aligned} \tag{2.11}$$

with $\mathbf{t}_{ij}$ being a normalized vector orthogonal to $\mathbf{n}_{ij}$ such that $(x_{ij}^1 - x_{ij}^0)\cdot\mathbf{t}_{ij} > 0$.

On boundary edges the numerical flux and the gradient reconstruction are defined analogously with proper management of the Dirichlet and Neumann conditions (cf. [3] for details).

2.3. Reduced Basis Method. We can write the FV scheme (2.9) in a more compact form as

$$\begin{aligned}&U_H^0(\mu) := P[u_0(x;\mu)] \\ &U_H^k(\mu) := U_H^{k-1}(\mu) + \Delta t L(t^k,\mu)[U_H^{k-1}], \qquad k = 1,\dots,K.\end{aligned} \tag{2.12}$$

Here, $P : \mathcal{W} \to \mathcal{W}_H$ is a projection onto the discretization space and $L(t,\mu) : \mathcal{W}_H \to \mathcal{W}_H$ is an explicit FV evolution operator. In this section only this more general notation is used and, therefore, the approach can also be applied to other discretizations and further parabolic problems fitting into this setting.

2.3.1. Empirical Interpolation of Evolution Operator. In order to construct an RB approximation of the problem (2.12), we need to assume that the operators can be written in an affinely decomposed form.

Definition 2.2. *The Finite Volume scheme (2.12) is affinely decomposed, if the operators P and L can be rewritten as*

$$\begin{aligned}P[u_0(x;\mu)] &= \sum_{q=0}^{Q_P} P^q(x)\sigma_P^q(\mu) \\ L(t,\mu)[U_H] &= \sum_{q=0}^{Q_L} L^q(t)[U_H]\sigma_L^q(t,\mu)[U_H],\end{aligned} \tag{2.13}$$

where P^q and L^q are linear operators that are independent of the parameter μ and the scalar functions $\sigma_P^q(\mu)$ and $\sigma_L^q(t,\mu)$ are computationally independent of the space variable x.

Obviously, the evolution operator we described in the last section 2.2 is not of the desired form. This is why we need to consider a collateral reduced basis (CRB) space $\mathcal{W}_M$ that is spanned by basis functions $\Xi_M := \{\xi_m\}_{m=1}^M$. The CRB basis functions are nodal functions which are equal to 1 at exactly one point of an interpolation point set $T_M := \{x_m\}_{m=1}^M$ and vanish on the others, i.e. $\xi_m(x_{m'}) = \delta_{m,m'}$ for all $m, m' = 1,\dots,M$. With these, we can compute a so-called empirical interpolation (EI) operator

$$\mathcal{I}_M[L(t,\mu)[U_H]] := \sum_{m=1}^M l_m(t,\mu)[U_H]\xi_m \quad \text{for all } U_H \in \mathcal{W}_H. \tag{2.14}$$

Here, the coefficient functions $l_m(t;\mu)[U_H]$ are point evaluations of the finite volume operator $L(t,\mu)$ in the interpolation points T_M. Computationally, these functions are determined simultaneously by a local finite volume operator evaluation on a subgrid with $M' \ll H$ cells. Due to the locality of the finite volume scheme (2.9), the constant M', which determines the computational complexity, is bounded by $M' \leq 9M$, because the fluxes over the edges of a cell require evaluations of U_H in the 8 neighbouring degrees of freedom. Due to construction, the EI operator coincides at the interpolation points with the evolution operator

$$\mathcal{I}_M[L(t,\mu)[U_H]](x_m) = L(t,\mu)[U_H](x_m) \quad \text{for all } m = 1,\dots,M. \tag{2.15}$$

As a result, if we substitute the operator L in (2.12) by its interpolant $\mathcal{I}_M[L]$, the Finite Volume scheme complies to the affinely decomposed form (2.13).

The construction of Ξ_M and T_M is done in an extensive search algorithm, where the basis functions are determined from a training set of snapshots

$$L_{\text{train}} := \left\{ L(t,\mu)[U_H^{k-1}(\mu)] \mid k = 1,\dots,K, \mu \in \mathcal{M} \right\}$$

with a finite parameter subset $\mathcal{M} \subset \mathcal{P}$. This algorithm works iteratively and picks in each step, the worst approximated snapshot from L_{train} and a corresponding interpolation point. Details of this construction are presented in [6], which is based on the original empirical interpolation method [1].

2.3.2. Reduced Basis Approximation. The CRB space $\mathcal{W}_M \subset \mathcal{W}_H$ for the EI of L is constructed such that it optimally approximates operator evaluations from the training set L_{train}. Analogously, we construct an RB space $\mathcal{W}_N \subset \mathcal{W}_H$ such that the projection error for a training set of discrete solutions

$$U_{\text{train}} := \left\{ U_H^k(\mu) \mid k = 0,\dots,K, \mu \in \mathcal{M} \right\}$$

becomes reasonably small: We initially choose an orthonormalization of the μ-independent functions $P^q(x)$ in (2.13) and incrementally add functions from the set U_{train} chosen by a greedy search algorithm. The resulting set after N steps, then gives us a basis for the RB space $\mathcal{W}_N$. The choice of the first vectors for the basis assures that initial solutions $U_H^0(\mu)$ are approximated with zero error which simplifies error analysis.

For details on the construction algorithm and error analysis used here, we again refer to [6]. A more sophisticated method using adaptive grids is given in [5].

Through substitution of L by its EI, the scheme 2.12 is of affinely decomposed form and can thus be projected onto $\mathcal{W}_N$. We arrive at the following definition, where we use $\langle \cdot, \cdot \rangle$ to denote the $L^2(\Omega)$ inner product on $\mathcal{W}_H$.

Definition 2.3 (Reduced basis scheme). *Let $\mathcal{W}_N \subset \mathcal{W}_H$ be a RB space spanned by basis functions $\{\varphi_n\}_{n=1}^N$ and $\mathcal{W}_M \subset \mathcal{W}_H$ be the CRB space for the EI of an explicit discretization operator $L(t^k,\mu)$. We further denote the interpolation points with $\{x_m\}_{m=1}^M$ and the corresponding nodal basis functions with $\{\xi_m\}_{m=1}^M$. Then for all $k = 0,\dots,K$ and $\mu \in \mathcal{P}$ the functions $U_N^k(\mu) := \sum_{n=1}^N a_n^k(\mu)\varphi_n$ with the coefficient vectors $\mathbf{a}^k := \left(a_0^k(\mu),\dots,a_N^k(\mu)\right)^t \subset \mathbb{R}^N$ are defined as the solution of the reduced basis scheme*

$$\begin{aligned} \mathbf{a}^0(\mu) &:= \left(\langle P[U_0(\mu)], \varphi_1 \rangle, \dots, \langle P[U_0(\mu)], \varphi_N \rangle\right)^t \\ \mathbf{a}^{k+1}(\mu) &:= \mathbf{a}_n^k(\mu) + \Delta t \mathbf{Bl}(\mu, t^k)[\mathbf{a}^k(\mu)] \end{aligned} \tag{2.16}$$

for $k = 1, \dots, K-1$. *Here the vector* $\mathbf{l}$ *and the matrix* $\mathbf{B}$ *are defined by*

$$(\mathbf{B})_{nm} := \langle \xi_m, \varphi_n \rangle \,, \tag{2.17}$$

$$(\mathbf{l}(t^k, \mu))_m := \mathcal{I}_M[L(t^k, \mu)[U_N^k(\mu)]](x_m) \tag{2.18}$$

for $n = 1, \dots, N$ *and* $m = 1, \dots, M$.

All the parameter-independent parts of this scheme can be precomputed in a possibly extensive offline phase. For varying parameters, the scheme can afterwards be computed very efficiently in the online phase as the complexity of these computations depends only polynomial on the dimensions of the reduced basis spaces N and M. Furthermore, rigorous a posteriori error estimates for the error $\|U_H^k(\mu) - U_N^k(\mu)\|_{L^2(\Omega)}$ can be computed equally efficiently in an offline/online way. For details, we refer to [7].

3. Numerical Experiments. The experiments are implemented in MATLAB and based on our package RBmatlab, that provides FV discretizations, algorithms for empirical interpolation, RB generation and RB simulations.

We consider a quadratic reference domain for which the upper border can be transformed to a parabolic segment, cf. Fig. 3.1d, depending on one parameter. The left and right borders are assigned Dirichlet boundary conditions, depending on a further parameter. The upper and lower border of the domain are natural no-flow boundaries. More precisely, we choose our reference domain to be $\hat{\Omega} := [0, 1]^2$

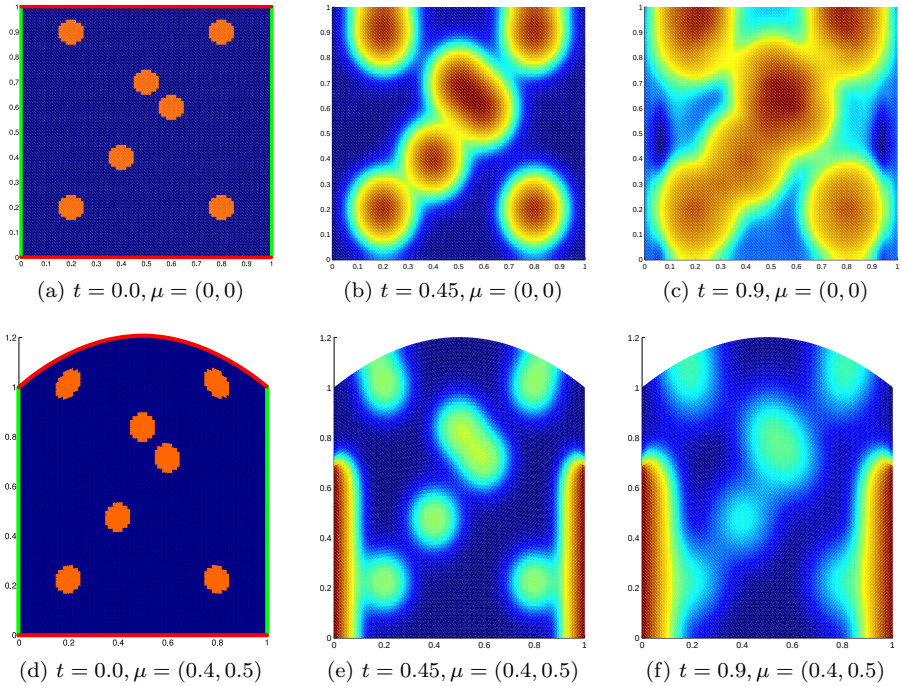

(a) $t = 0.0, \mu = (0, 0)$ (b) $t = 0.45, \mu = (0, 0)$ (c) $t = 0.9, \mu = (0, 0)$

(d) $t = 0.0, \mu = (0.4, 0.5)$ (e) $t = 0.45, \mu = (0.4, 0.5)$ (f) $t = 0.9, \mu = (0.4, 0.5)$

Fig. 3.1: Illustration of the numerical solution for different parameters and times. Subfigures (a) and (d) have highlighted left and right Dirichlet (green) and upper and lower Neumann (red) boundaries.

and the geometry transformation as $\Phi(\hat{x};\mu) := (\hat{x}_1, \hat{x}_2 \cdot (-4\mu_1\hat{x}_1^2 + 4\mu_1\hat{x}_1))^t$, with $\mu = (\mu_1, \mu_2)$ in the parameter domain $\mathcal{P} := [0, 0.4] \times [0, 0.5]$. The initial data function $u_0(\hat{x};\mu) := \sum_{i=1}^{7} 0.2\chi_{\{(\hat{x}-b_i)^2<0.05\}}$ is built as a sum of seven indicator functions on circles with centres $b_i \in \mathbf{R}^2, i = 1, \ldots, 7$. Note that u_0 is defined on the reference domain, such that after the geometry transformation the circles turn into ellipses, cf. Figure 3.1d. Otherwise the required affine decomposition property of the initial data u_0 would a priori not be satisfied. Indeed, with an additional empirical interpolation step it would be possible to bring the function u_0 into the desired affine form, but this would result in an additional approximation error.

On the left and the right domain boundaries we assign Dirichlet values $g_D(x, t;\mu) := \mu_2\chi_{\{x_2>0.7\}}$. The computations are run on a 100×80 grid with fixed end time $T_{\max} = 0.9$ and the time-interval is divided into $K := 300$ intervals such that stability of the evolution scheme is guaranteed for all $\mu \in \mathcal{P}$.

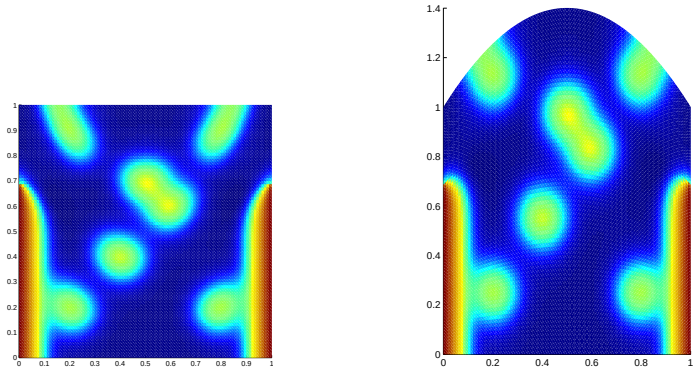

(a) $\hat{\Omega}$ (b) Ω

Fig. 3.2: Illustration of the solution snapshot $U_H^k(\mu)$ with $k = 150$ and $\mu = (0.25, 0.4)$ on the reference domain (a) and the actual domain (b). In (a) the anisotropic diffusion on the reference domain is visible.

Figure 3.1 shows solutions for different parameter combinations and times. The diffusion process in time is visible from left to right on a non-deformed domain for $\mu = (0, 0)$ and a deformed domain for $\mu = (0.4, 0.5)$. In both cases we observe the expected isotropic diffusion on Ω. Figure 3.2 presents a specific solution snapshot on the reference domain $\hat{\Omega}$ and the deformed domain Ω. We can clearly observe the anisotropy of the diffusion on the reference domain.

The CRB space $\mathcal{W}_M$ has $M := 50$ basis functions that are extracted from the set of snapshots L_{train}, where the underlying finite subset of the parameter space $\mathcal{M} \subset \mathcal{P}$ consists of 16 uniformly distributed points. The parameters and time indices of the snapshots which the EI algorithm selects can be seen in Fig. 3.3a. The gray-shades indicate the order of the selection, i.e. darker points indicate earlier selected snapshots.

We clearly observe that the most important snapshots are selected for the extreme values of the second parameter, i.e. the Dirichlet parameter. This is understandable as with the linearity of the equation, every solution $U_H^k(\mu)$ for $\mu = (\mu_1, \mu_2) \in \mathcal{P}$ formally is a convex combination of the solutions $U_H^k((\mu_1, 0))$ and $U_H^k((\mu_1, 0.5))$. The EI-selection procedure therefore correctly discovers this importance of the extreme solutions. The first parameter, i.e. the geometry transformation, has a stronger effect

on the operator than Dirichlet boundary data, especially for low time indices and large geometry distortions.

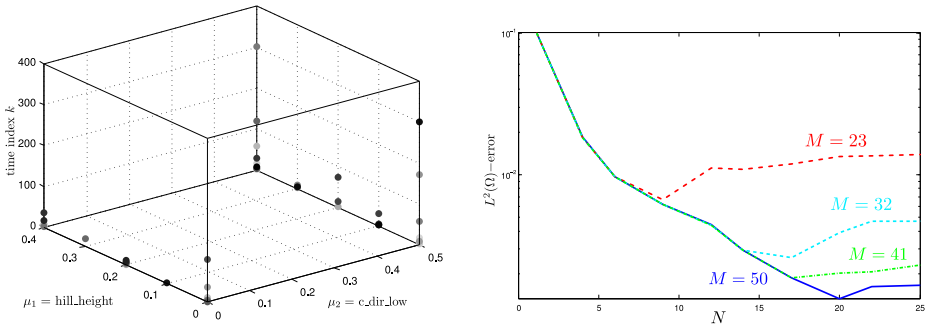

(a) (b)

Fig. 3.3: (a) Parameters and time indices of selected snapshots for basis functions of CRB space. (b) RB error convergence on 100 test samples for growing basis size N at different CRB dimensions M.

The same set $\mathcal{M}$ is used in order to build the RB space $\mathcal{W}_N$ which is spanned by $N := 25$ basis functions. Figure 3.3b illustrates the error convergence for different reduced approximations. For this purpose, we use a set $\mathcal{M}_{\text{test}} \subset \mathcal{P}$ of 100 randomly chosen test parameters. Then we plot the error

$$\max_{k=0,\dots,K} \max_{\mu \in \mathcal{M}_{\text{test}}} \left\| U_H^k(x;\mu) - U_N^k(x;\mu) \right\|_{L^2(\Omega)}$$

for growing RB dimension N and for different fixed CRB dimensions. For coarse operator approximations like e.g. $M = 23$, we observe that the error induced by the EI dominates and the RB approximation error cannot drop below a certain level.

The main goal of the RB method is to reduce the simulation time. Table 3.1 gives an overview of the runtime gain for varying dimensions of the reduced spaces. As the construction of the RB space and collateral RB space with $N = 25$ and $M = 50$ took altogether about 2920 sec. and the time gain per simulation at this configuration is about 18.5 sec., we get a total time gain if more than 160 different simulations need to be computed. Note, however, that this "break even point" will get smaller if the dimensionality of $\mathcal{W}_H$ is increased.

4. Conclusion. We have shown that RB methods for finite volume schemes [6, 7] can be used for parametrized geometries. The crucial ingredients are i) a reference mapping of the equation onto a reference domain, ii) a finite volume scheme with correct treatment of non-isotropic diffusion tensors by gradient reconstruction, iii) an empirical interpolation of the resulting finite volume space discretization operator and iv) a reduced basis approximation for the FV scheme. Experimentally, we have demonstrated a considerable acceleration of the online simulations.

As expected, the explicit discretization of diffusivities leads to small time-steps, hence is only applicable for small diffusivities. This can obviously be improved by extending the RB-method with implicit operator components. We would expect a considerably larger acceleration in these cases, as the implicit time stepping in $\mathcal{W}_H$ will be much more expensive than the explicit steps in the current scheme.

Dimensions	Runtime[s]	max error
$H = 8000$	23.0626	0
$N = 1, \quad M = 1$	3.7714	0.612030
$N = 9, \quad M = 34$	4.3052	0.005632
$N = 9, \quad M = 50$	4.5438	0.005616
$N = 17, \ M = 34$	4.3081	0.002640
$N = 17, \ M = 50$	4.5474	0.001784
$N = 25, \ M = 34$	4.3142	0.004379
$N = 25, \ M = 50$	4.5497	0.001340

Table 3.1: Runtime comparisons for reduced and detailed simulations at varying dimensions of the reduced spaces.

RB approaches with FEM discretization frequently use domain decomposition and piecewise affine reference mappings. Consistency requirements of the numerical fluxes make this approach nontrivial for finite volume discretizations. Hence, this could be an interesting point for further research. Error quantification can be realized by implementing corresponding a posteriori error estimators [3].

Acknowledgement. Bernard Haasdonk was funded by the German Federal Ministry of Education and Research under grant number 03SF0310C and by the Landesstiftung Baden-Württemberg gGmbH.

REFERENCES

[1] M. Barrault, Y. Maday, N.C. Nguyen, and A.T. Patera. An 'empirical interpolation' method: application to efficient reduced-basis discretization of partial differential equations. *C. R. Math. Acad. Sci. Paris Series I*, 339:667–672, 2004.

[2] O. Drblíková and K. Mikula. Convergence analysis of finite volume scheme for nonlinear tensor anisotropic diffusion in image processing. *SIAM J. Numer. Anal.*, 46(1):37–60, 2007.

[3] M. Drohmann. Reduzierte Basis Methode für die Richards Gleichung. Master's thesis, Institut für Numerische und Angewandte Mathematik, Universität Münster, 2008. In Vorbereitung.

[4] R. Eymard, T. Gallout, and R. Herbin. A cell-centred finite volume approximation for anisotropic diffusion operators on unstructured meshes in any space dimension. *IMA Journal of Numerical Analysis*, 26(2):326–353, 2005.

[5] B. Haasdonk and M. Ohlberger. Adaptive basis enrichment for the reduced basis method applied to finite volume schemes. In *Proc. 5th International Symposium on Finite Volumes for Complex Applications*, pages 471–478, 2008.

[6] B. Haasdonk and M. Ohlberger. Reduced basis method for finite volume approximations of parametrized linear evolution equations. *M2AN, Math. Model. Numer. Anal.*, 42(2):277–302, 2008.

[7] B. Haasdonk, M. Ohlberger, and G. Rozza. A reduced basis method for evolution schemes with parameter-dependent explicit operators. Technical Report 09/07 - N, FB 10, University of Münster, 2007. Accepted by ETNA.

[8] A.T. Patera and G. Rozza. *Reduced Basis Approximation and a Posteriori Error Estimation for Parametrized Partial Differential Equations*. MIT, 2007. Version 1.0, Copyright MIT 2006-2007, to appear in (tentative rubric) MIT Pappalardo Graduate Monographs in Mechanical Engineering.

[9] C. Prud'homme, D. Rovas, K. Veroy, and A.T. Patera. A mathematical and computational framework for reliable real-time solution of parametrized partial differential equations. *M2AN Math. Model. Numer. Anal.*, 36(5):747–771, 2002.

[10] G. Rozza. *Shape design by optimal flow control and reduced basis techniques: Applications to bypass configurations in haemodynamics*. PhD thesis, École Polytechnique Fédérale de Lausanne, November 2005.